ISSUE: August 2025

Operational Transconductance Amplifiers In PWM ICs: Grounded And Negative Feedback Compensation Both Have Their Place

by Alain Laprade, Power Electronics Specialist, Saunderstown, R.I.

Operational transconductance amplifiers (OTAs) are commonly used with grounded-feedback compensation networks in PWM IC designs. However, an alternative configuration—connecting the compensation network via negative feedback to the output voltage divider—has shown promising results.[1,4] Despite its potential, this approach remains underutilized, likely due to misconceptions about its viability.

When I first experimented with this technique years ago as a field applications engineer, the prevailing belief was that OTA negative feedback wouldn't work. This article aims to clarify that misunderstanding and explore the merits of both configurations.

Using type-II feedback transfer function models, we'll compare grounded and negative-feedback implementations to highlight their respective tradeoffs and performance characteristics. All theoretical expressions are validated through SIMPLIS simulations to ensure practical relevance.

Background On OTA Compensation Networks

Grounded compensation OTA networks are well documented.[2] However, there are some lesser-known aspects of these networks. In particular, ICs requiring external compensation have an internal ESD protection structure and a parasitic capacitance (R_{esd} and C_0) located between the package pinout and the internal feedback OTA control signal (Fig. 1) which are not normally described in datasheets. Detailed grounded compensation OTA expressions describing the feedback control signal are presented in reference [3].

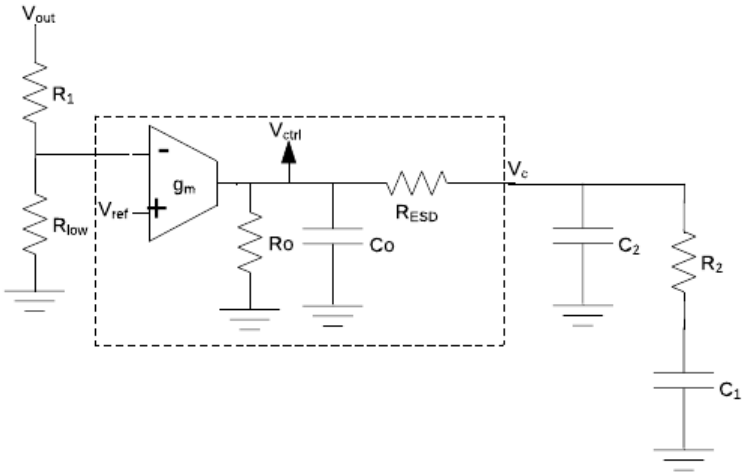

Fig. 1. Type-II OTA with grounded compensation network.

Output parasitic capacitance C_O introduces a high-frequency pole. R_{esd} introduces an upper mid-band frequency zero. For low R_2 resistance values, ($R_2 < \sim 5 \cdot R_{esd}$), use of R_2 to set the mid-band gain is limited and feedback loop measurements (OTA response, control-to-output response) begin introducing measurement errors as signals V_{ctrl} (the control loop signal) and V_c (the external IC measurement point) begin to diverge. Open-loop response in closed-loop form remains unchanged.

The ESD resistance introduces a limitation on compensation values and/or performance tradeoffs in applications such as automotive battery-connected boost and SEPIC topologies.

Now, let's considered the alternative of the negative-feedback compensation network. When a voltage error amplifier feedback network is connected using a negative-feedback configuration, the positive terminal is connected to a voltage reference, rendering the negative terminal as a virtual ground in the gain small-signal transfer function.

However, when an OTA compensation is configured as negative feedback (Fig. 2), the negative terminal virtual ground is lost. Voltage feedback divider resistor R_{low} is present in the error amplifier ac gain transfer function and attenuates mid-band gain. Larger R_2 values are used when targeting similar ac transfer function responses as their grounded-feedback counterparts. This overcomes design limitations from the Fig. 1 grounded-feedback configuration by providing greater control of midband gain.

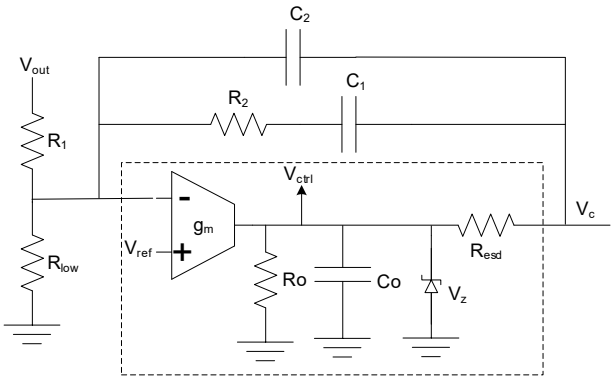

Fig. 2. Type-II OTA with negative-feedback configuration.

In the next section, expressions for the grounded type-II OTA transfer function derived in reference [3] will be summarized. Then, similar expressions for the negative-feedback compensation network are described in a subsequent section. These expressions are then used to compare grounded versus negative-feedback compensation. We then validate these expressions with simulations in the final sections.

Type-II Expressions For A Ground-Referenced Compensation Network

Type-II ground-referenced compensation network OTA expressions shown in Fig. 1 were developed in [3]. The OTA gain may be expressed as a third-order polynomial expression (1).

$$G_{gnd}(s) = -G_0 \frac{1+a_{1\_gnd}s+a_{2\_gnd}s^2}{1+b_{1\_gnd}s+b_{2\_gnd}s^2+b_{3\_gnd}s^3} \qquad (1)$$

Coefficients may be expressed as

$$a_{1\_gnd} = (R_2 + R_{esd})C_1 + R_{esd}C_2 \approx (R_2 + R_{esd})C_1 \qquad (2)$$

$$a_{2\_gnd} = R_2 R_{esd} C_1 C_2 \qquad (3)$$

$$b_{1_{gnd}} = R_0 C_0 + (R_0 + R_2 + R_{esd})C_1 + (R_0 + R_{esd})C_2$$

$$\approx (R_0 + R_2 + R_{esd})C_1 + (R_0 + R_{esd})C_2 \qquad (4)$$

$$b_{2\_gnd} = R_0(R_2 + R_{esd})C_0C_1 + R_0R_{esd}C_0C_2 + R_2(R_0 + R_{esd})C_1C_2$$

$$\approx R_0(R_2 + R_{esd})C_0C_1 + R_2(R_0 + R_{esd})C_1C_2 \qquad (5)$$

$$b_{3\_gnd} = R_0 R_{esd} R_2 C_0 C_1 C_2 \qquad (6)$$

For well-separated poles and zeros, the expression (1) quality factor Q is << 1 and may be simplified as cascaded 1st-order terms as in expression (7).

$$G_{gnd}(s) \approx -G_0 \frac{\left(1+\frac{s}{\omega_{z1\_gnd}}\right)\left(1+\frac{s}{\omega_{z2\_gnd}}\right)}{\left(1+\frac{s}{\omega_{p1\_gnd}}\right)\left(1+\frac{s}{\omega_{p2\_gnd}}\right)\left(1+\frac{s}{\omega_{p3\_gnd}}\right)} \quad (7)$$

where

$$G_0 = \frac{R_{low}}{R_{low}+R_1} g_m R_0 \quad (8)$$

$$\omega_{z1\_gnd} = \frac{1}{a_{1\_gnd}} = \frac{1}{(R_2+R_{esd})C_1} \quad (9)$$

$$\omega_{z2\_gnd} = \frac{a_{1\_gnd}}{a_{2\_gnd}} = \frac{1}{(R_2 \| R_{esd})C_2} \quad (10)$$

$$\omega_{p1\_gnd} = \frac{1}{b_{1\_gnd}} = \frac{1}{(R_0+R_2+R_{esd})C_1+(R_0+R_{esd})C_2} \quad (11)$$

$$\omega_{p2\_gnd} = \frac{b_{1\_gnd}}{b_{2\_gnd}} = \frac{(R_0+R_2+R_{esd})C_1+(R_0+R_{esd})C_2}{R_0(R_2+R_{esd})C_0C_1+R_2(R_0+R_{esd})C_1C_2} \quad (12)$$

$$\omega_{p3_{gnd}} = \frac{b_{2_{gnd}}}{b_{3_{gnd}}} = \frac{R_0(R_2+R_{esd})C_0C_1 + R_2(R_0+R_{esd})C_1C_2}{R_0R_{esd}R_2C_0C_1C_2}$$

$$\approx \frac{R_2(R_0+R_{esd})}{R_0R_{esd}R_2C_0} \quad (13)$$

To determine the compensation value expressions, we must first express the magnitude of $G_{gnd}(s)$ at a selected crossover frequency f_c.

$$G_{fc\_gnd} \approx -G_0 \frac{\sqrt{1+\left(\frac{f_{z1}}{f_c}\right)^2}}{\sqrt{1+\left(\frac{f_c}{f_{p1}}\right)^2}}$$

$$= -\frac{R_{low}}{R_{low}+R_1} g_m R_0 \frac{\omega_{p1\_gnd}}{\omega_{z1\_gnd}} \quad (14)$$

From expressions (8), (9), and (10) we now determine the compensation network component values.

$$R_2 = \frac{R_{low}+R_1}{R_{low}} \frac{\left|G_{fc_{gnd}}\right|}{g_m} - R_{esd} \quad (15)$$

$$C_1 = \frac{1}{\omega_{z1_{gnd}}(R_2+R_{esd})} \quad (16)$$

$$C_2 = \frac{1}{\omega_{z2_{gnd}}(R_2 \| R_{esd})} \quad (17)$$

To validate the similarity of the exact and simplified expressions, desired pole/zero values are provided in Table 1. Component parametric values are from onsemi's PWM IC NCV887103.[5] Table 2 lists chosen compensation component values. The resulting OTA transfer function is plotted in Fig. 3.

Table 1. Desired pole and zeroes.

g_m	0.00107 Ω^{-1}	NCV887103
R_0	3 MΩ	NCV887103
C_0	10 pF	NCV887103
R_{esd}	542 Ω	NCV887103
f_{z1}	350 Hz	
f_{p2}	37 kHz	

Table 2. Component values for the grounded compensation network.

	Calculated	Selected
R_1		53.6 kΩ
R_{low}		2.61 kΩ
C_1	46.98 nF	47 nF
R_2	8.958 kΩ	9.09 kΩ
C_2	470.2 pF	470 pF
f_{z2}	650 kHz	N/A
f_{p3}	19 MHz	N/A

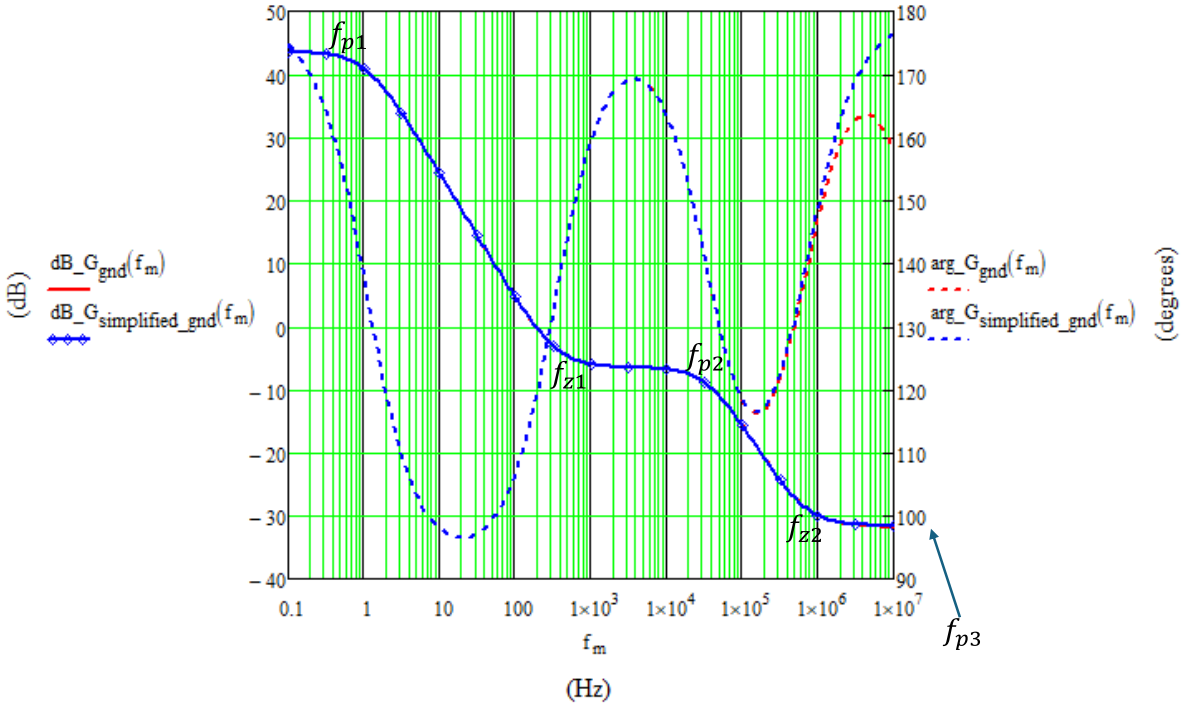

Fig. 3. Ground-referenced OTA transfer function.

The simplified transfer function matches the exact expression up to ~1 MHz, well beyond the maximum switching frequency of the NCV8871 family (340 kHz). The expressions remain meaningful for a similar NCV898031 2-MHz device.[6]

Type-II Expressions For A Negative-Feedback Compensation Network

It has been shown that OTAs may be used in negative-feedback configuration.[1,4] The type-II poles and zeroes are now derived. Tradeoffs between the two compensation methods are evaluated in an example.

The virtual ground is lost with OTAs having negative feedback compensation because of the transconductance (g_m) voltage-dependent current source. The transfer function from Fig. 2 (repeated here for the reader's convenience) may be expressed as a third-order polynomial transfer function in expression (18).

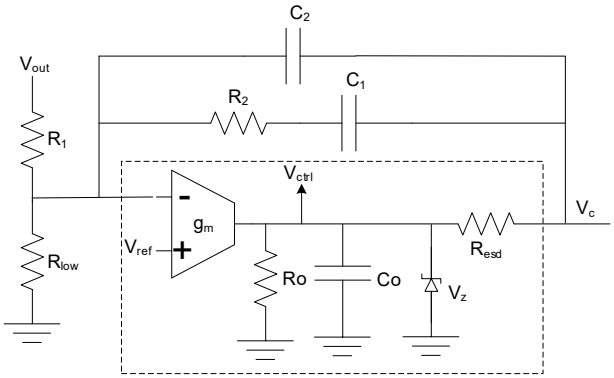

Fig. 2 again. Type-II OTA with negative-feedback configuration.

$$G_{neg}(s) = -G_0 \frac{\left(1+\frac{s}{\omega_{z1\_neg}}\right)\left(1-\frac{s}{\omega_{z2\_neg}}\right)}{1+b_{1\_neg}s+b_{2\_neg}s^2+b_{3\_neg}s^3} \quad (18)$$

$$\omega_{z1\_neg} = \frac{1}{(R_2+R_{esd}-\frac{1}{g_m})C_1} \quad (19)$$

$$\omega_{z2\_neg} = \frac{1}{(R_{esd}-\frac{1}{g_m})C_2} \quad (20)$$

$$b_{1_{neg}} = (R_0 + R_2 + R_{esd} + (1 + \mathrm{g_m}R_0)(R_1 \parallel R_{low}))C_1$$

$$+ (R_0 + R_{esd} + (1 + \mathrm{g_m}R_0)(R_1 \parallel R_{low}))C_2 + R_0C_0$$

$$\approx (R_0 + (1 + g_m(R_1 \parallel R_{low})))(C_1 + C_2) \quad (21)$$

$$R_A = R_0 + R_2 + R_{esd} + (1 + g_mR_0)(R_1 \parallel R_{low}) \quad (22)$$

$$\mathrm{R_B} = R_0 + R_{esd} + (1 + \mathrm{g_m}R_0)(R_1 \parallel R_{low}) \quad (23)$$

$$\mathrm{R_C} = \frac{R_2+R_{esd}+(R_1\|R_{low})}{1+\mathrm{g_m}(R_1\|R_{low})} \quad (24)$$

$$R_D = \frac{R_{esd}+(R_1\|R_{low})}{1+g_m(R_1\|R_{low})} \quad (25)$$

$$b_{2\_neg} = R_AC_1((R_B \parallel R_2)C_2 + (R_C \parallel R_0)C_0) + R_BC_2(R_D \parallel R_0)C_0$$

$$\approx (R_0 + (1 + \mathrm{g_m}(R_1 \parallel R_{low})))R_2C_1C_2 \quad (26)$$

$$b_{3\_neg} = R_A(R_B \parallel R_2)(R_D \parallel R_0)C_0C_1C_2$$

$$\approx R_0(1 + \mathrm{g_m}(R_1 \parallel R_{low}))R_2(\frac{R_{esd}+(R_1\|R_{low})}{1+\mathrm{g_m}(R_1\|R_{low})})C_0C_1C_2 \quad (27)$$

For well-separated poles, $G_{neg}(s)$ may be simplified.

$$G_{neg}(s) \approx -G_0 \frac{\left(1+\frac{s}{\omega_{z1\_neg}}\right)\left(1+\frac{s}{\omega_{z2\_neg}}\right)}{\left(1+\frac{s}{\omega_{p1\_neg}}\right)\left(1+\frac{s}{\omega_{p2\_neg}}\right)\left(1+\frac{s}{\omega_{p3\_neg}}\right)} \quad (28)$$

where

$$\omega_{p1\_neg} = \frac{1}{b_{1\_neg}} = \frac{1}{(R_0+(1+g_m(R_1\|R_{low})))(C_1+C_2)} \quad (29)$$

$$\omega_{p2\_neg} = \frac{b_{1\_neg}}{b_{2\_neg}} = \frac{1}{R_2(C_1\|C_2)} \quad (30)$$

$$\omega_{p3\_neg} = \frac{b_{2\_neg}}{b_{3\_neg}} = \frac{1+\mathrm{g_m}(R_1\|R_{low})}{(R_{esd}+(R_1\|R_{low}))C_0} \quad (31)$$

To establish compensation component values, we must first express the magnitude of $G_{neg}(s)$ at the same crossover frequency f_c as that of the grounded compensation network (14) from the section above.

$$G_{fc\_\mathrm{neg}} = G_{fc\_\mathrm{gnd}} \quad (32)$$

From expressions (29), (30) and (31),

$$R_2 = R_0\left(1 + \mathrm{g_m}(R_1 \parallel R_{low})\right)\frac{\omega_{p1\_neg}}{\omega_{z1\_neg}} - R_{esd} + \frac{1}{\mathrm{g_m}} \quad (33)$$

$$C_1 = \frac{1}{\omega_{p1\_neg}R_0\left(1+\mathrm{g_m}(R_1\|R_{low})\right)} \quad (34)$$

$$C_2 = \frac{1}{R_2\omega_{p1\_neg}} \quad (35)$$

To verify the similarity between the exact and simplified expressions, we reuse the same pole/zero frequencies from that of Table 1. The resulting transfer function compensation component values (C_1, R_2, C_2) are summarized in Table 3 and plotted in Fig. 4. The value for f_{z2} is negative, indicative of a high-frequency right-hand-plane zero (RHPZ) that is dependent on compensation capacitor C_2.

The RHPZ introduces phase lag at $f_{z2}/10$ (340 kHz) that may be detrimental for a high-bandwidth design's minimum objective for feedback loop phase margin (typically 45° to 60° as a general practice).

Table 3. Component values for the negative-feedback compensation network.

	Calculated	Selected
R_1		53.6 kΩ
R_{low}		2.61 kΩ
C_1	12.2 nF	12 nF
R_2	37.8 kΩ	38.3 kΩ
C_2	114 pF	120 pF
f_{z2}	-3.4 MHz	N/A
f_{p3}	19 MHz	N/A

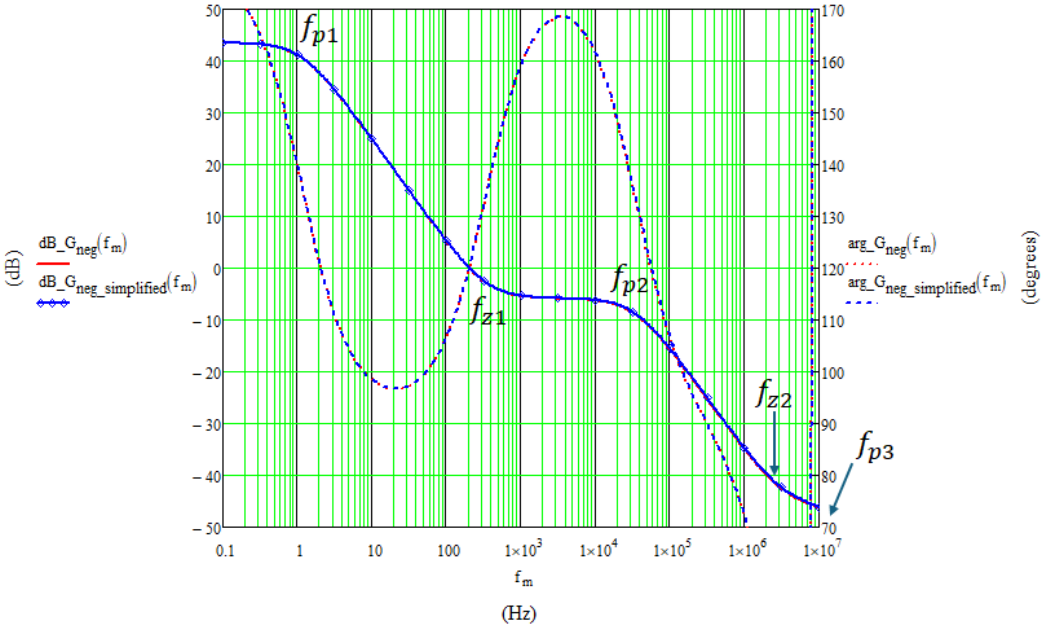

Fig. 4. Negative-feedback OTA transfer function.

Both simplified and exact transfer functions match in a useful range well beyond the maximum switching frequency of 2-MHz controllers.[6]

Comparison Of Grounded Versus Negative-Feedback OTA Compensation

Fig. 5 overlays OTA compensation for grounded and negative-feedback compensation networks for examples from the prior section. With each network, the ESD structure's (R_{esd} and C_0) influence on the transfer function manifests itself differently at high frequency. Depending on the design compensation requirements, the compensation methods have tradeoffs.

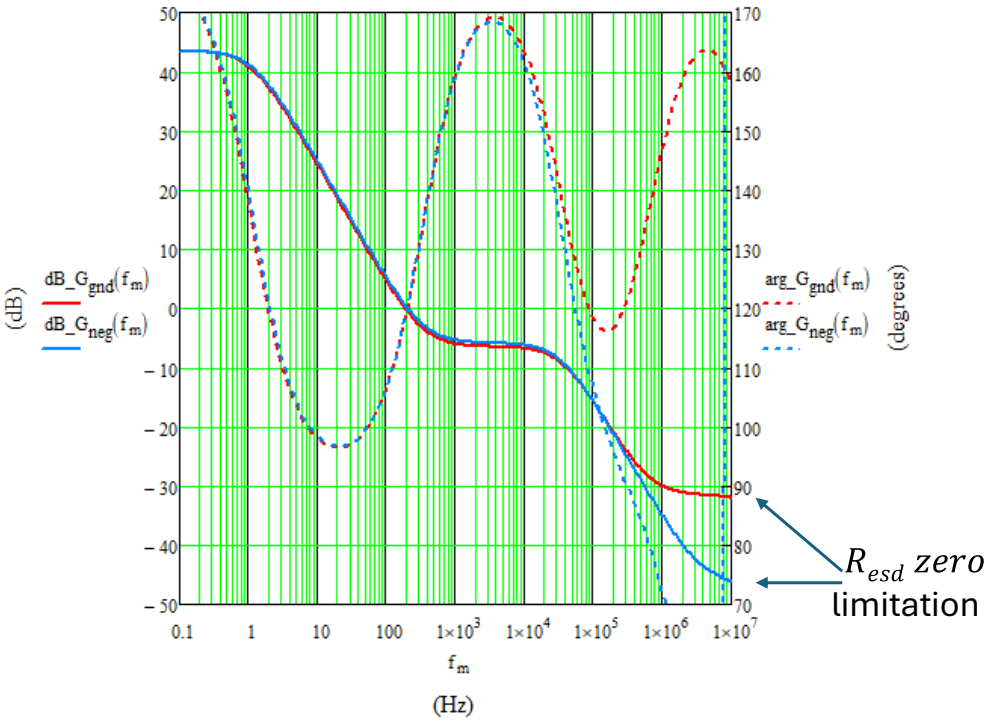

Fig. 5. OTA compensation comparison: grounded versus negative feedback.

Derived compensation expressions are verified using SIMPLIS with small-signal models from Fig. 6. Simulation results are shown in Fig. 7.

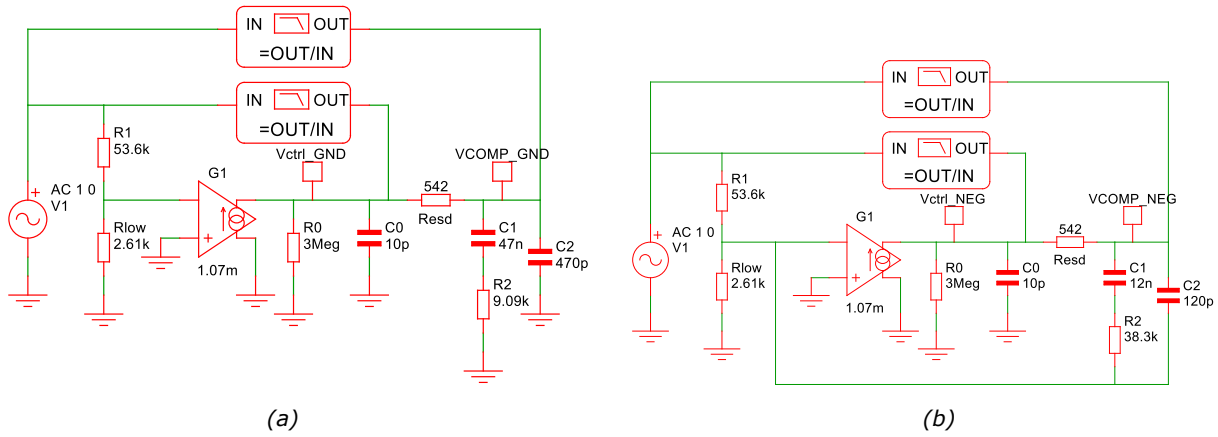

Fig. 6. SIMPLIS OTA grounded (a) and negative feedback (b) boost converter models.

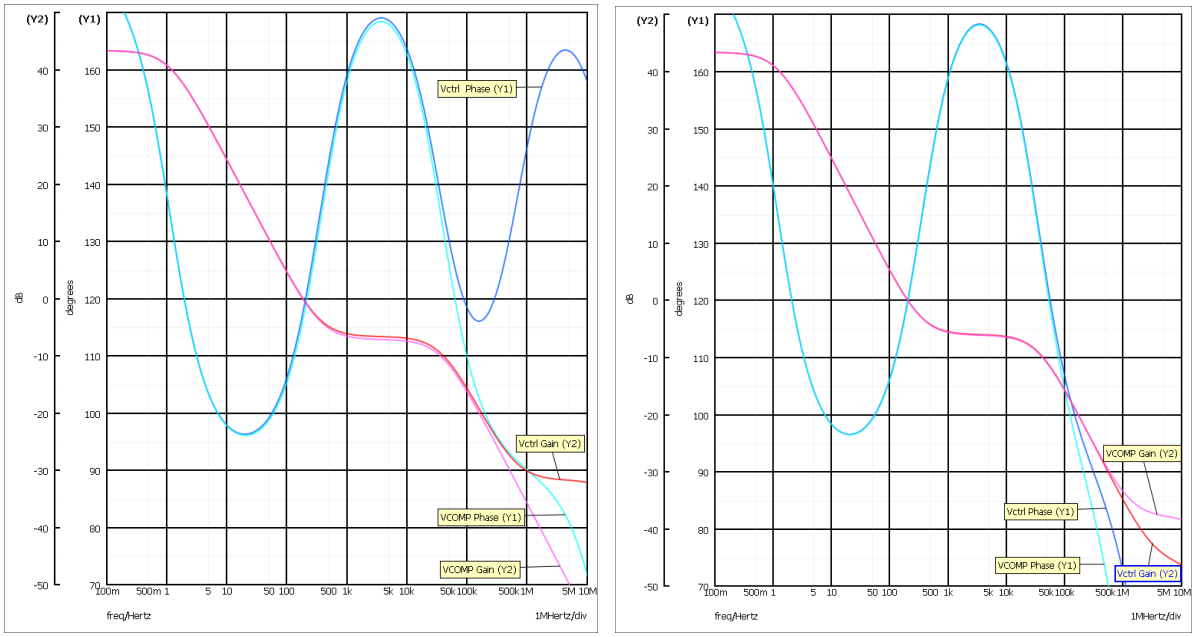

(a) *(b)*

Fig. 7. SIMPLIS OTA grounded (a) and negative feedback (b) small-signal responses.

The merits of each compensation methods differ and are summarized in Table 4.

Table 4. Comparison of compensation methods.

	Advantage	Disadvantage
Grounded compensation	R_{esd} introduces a high-frequency zero (ω_{z2_gnd}) which provides a high-frequency phase boost. This facilitates higher-bandwidth systems having good phase margin.	In designs where the PWM IC's slope compensation is low for the inductor's ripple current, it may be necessary to reduce the OTA mid-band gain significantly with a low R_2 compensation resistor value to help achieve adequate closed-loop attenuation at half the switching frequency so as to prevent sub-harmonic oscillation. This can be challenging when done in conjunction with higher-ESR output filter capacitors. R_{esd} limits the high-frequency OTA gain roll-off to a set value irrespective of the value of compensation resistor R_2.
Negative-feedback compensation	Larger R_2 compensation resistor values are used to shape the same mid-band gain frequency response. R_{esd} has significantly less influence on the minimum high-frequency gain.	A high-frequency right-half plane zero (ω_{z2_gnd}) is introduced, making it more challenging to achieve a sufficient phase margin in designs requiring a high-bandwidth closed-loop response.

Boost Converter Example

Compensation values introduced in Table 2 were used for a boost converter design supported by this author which used the NCV887103 PWM controller. A design requirement was to have the ability for startup at a

minimum automotive battery voltage of 6 V for a 26-V output having a 43.3-Ω resistive load. The Fig. 8 schematic is representative of the design's power stage. Table 2 compensation component values were used.

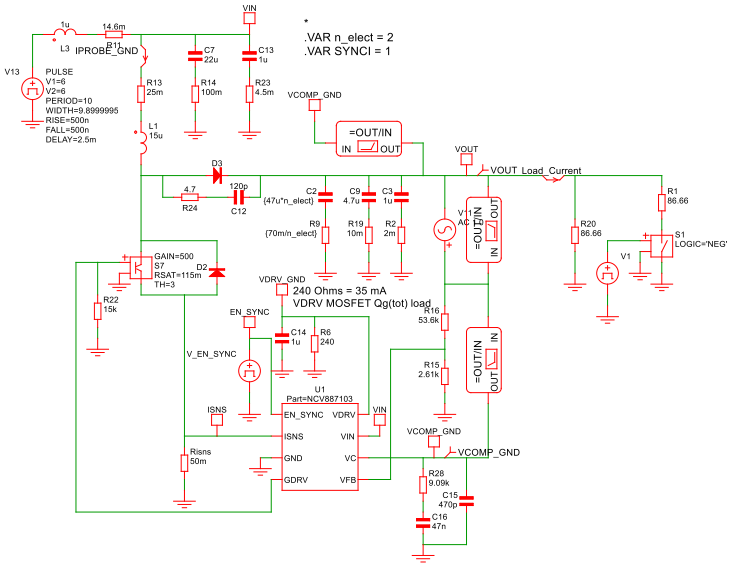

Fig. 8. A 26-V output boost converter with grounded-feedback compensation.

Startup and 100-to-50-to-100% load transient waveforms are displayed in Fig. 9.

Current-limit during startup results in ~0.5-V output overshoot during startup. This is a result of a large-signal effect caused by the OTA output voltage saturation (~2.3 V), resulting in stored charge in compensation capacitors C15 and C16. The 50-to-100-to-50% load transient results in a 26-mV peak-peak output voltage.

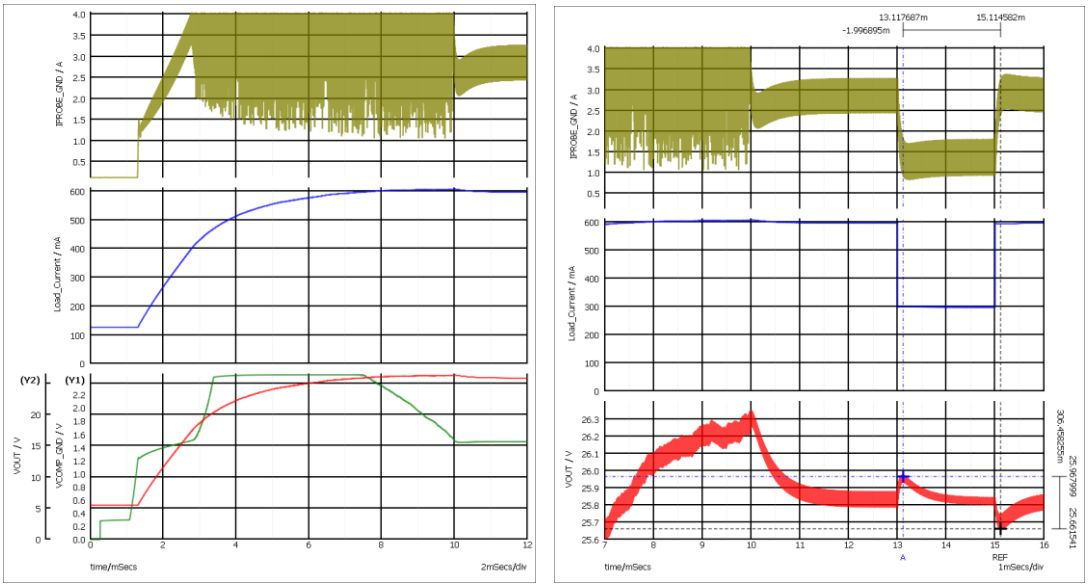

(a) *(b)*

Fig. 9. Grounded-feedback-compensation boost converter startup (a) and 50% load transient (b) responses.

The open-loop response in closed-loop form is plotted in Fig. 10. The crossover frequency is 2.9 kHz, having a gain margin of 16.5 dB and phase margin of 72.8°.

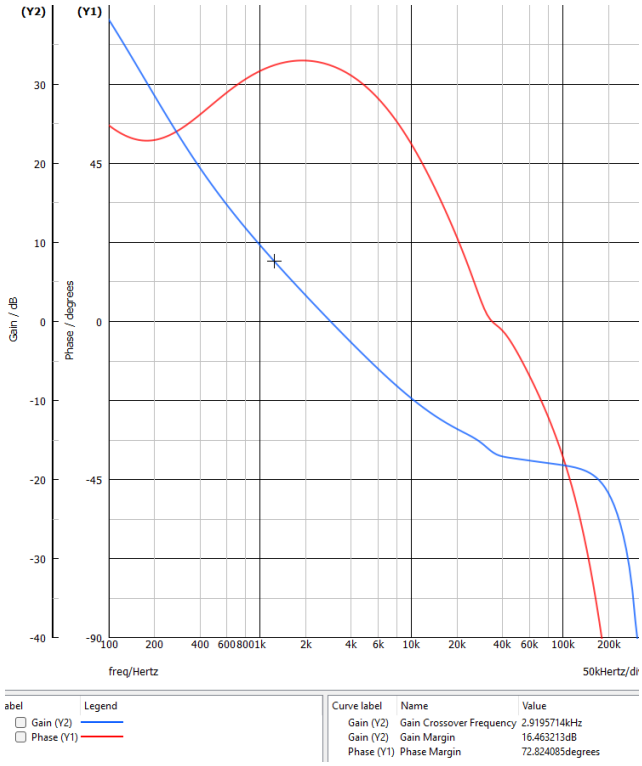

Fig. 10. Open-loop response in closed-loop form—grounded compensation.

Table 3 compensation values are now used to implement a similar bandwidth design using a negative compensation network (Fig. 11).

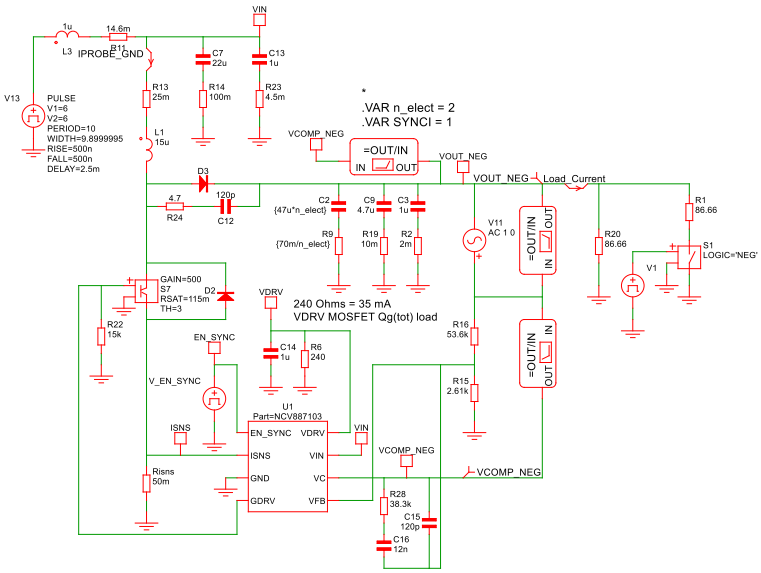

Fig. 11. A 26-V output boost converter with negative-feedback compensation.

Start-up and 100-to-50-to-100% load transient waveforms are displayed in Fig. 12. The startup overshoot voltage amplitude and the peak-to-peak voltage transient response are nearly identical to that of the grounded compensation configuration.

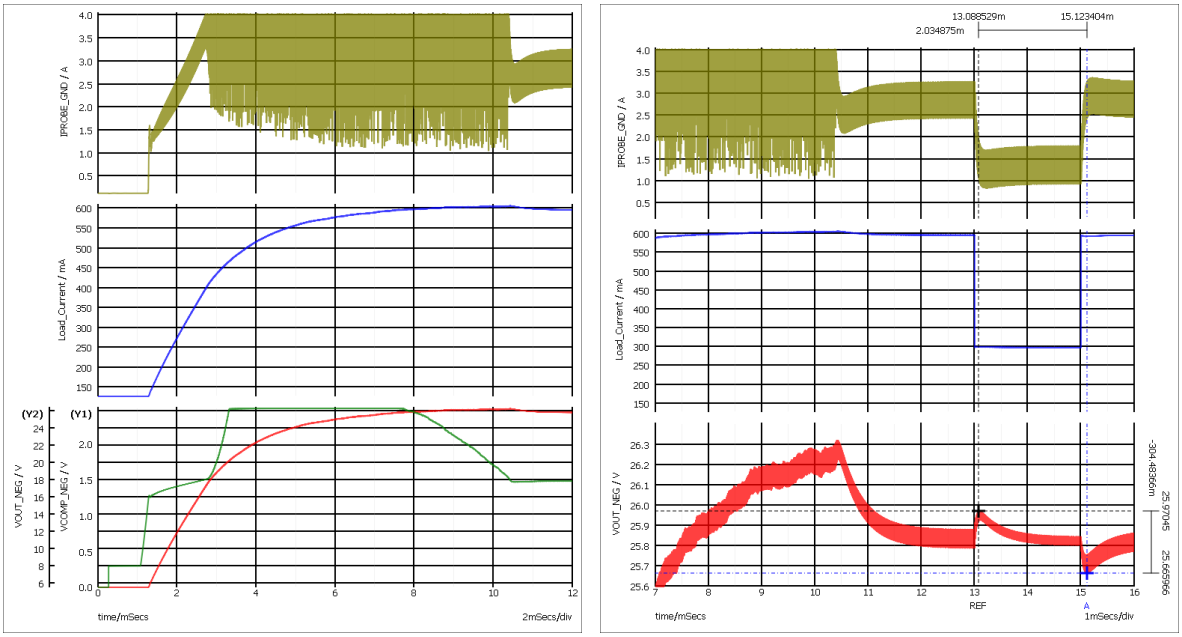

Fig. 12. Negative-feedback-compensation boost converter startup (a) and 50% load transient (b) responses.

The open-loop response in closed-loop form is plotted in Fig. 13. The crossover frequency is 3.1 kHz with a gain margin of 15.1 dB and phase margin of 71.7°.

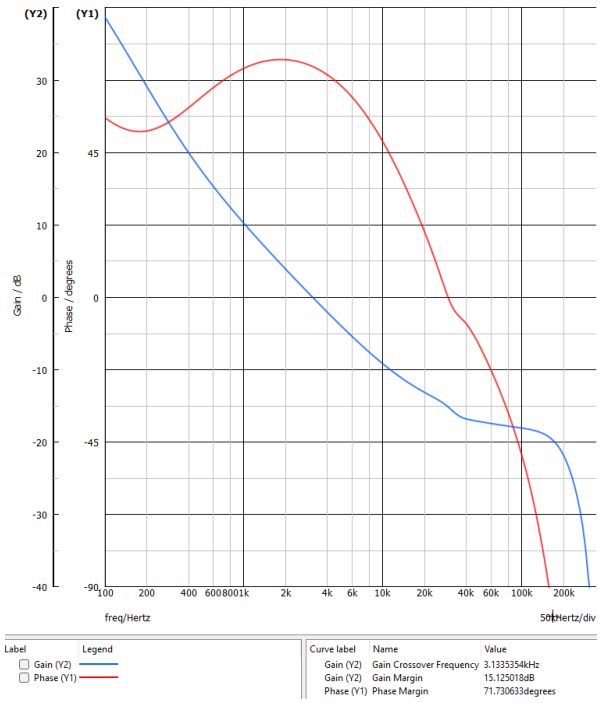

Fig. 13. Open-loop response in closed-loop form—negative-feedback compensation.

Conclusion

This analysis has demonstrated that both grounded and negative-feedback compensation configurations for OTAs present viable options for designing stable, efficient control loops in PWM applications. Grounded compensation networks benefit from a high-frequency phase boost introduced by R_{esd}, enabling robust phase margins in high-bandwidth systems. However, this configuration may face challenges in managing sub-harmonic oscillations when low mid-band gain (R_2) values are required for systems having insufficient slope compensation.

In contrast, negative-feedback configurations allow greater flexibility in shaping mid-band gain and mitigating the high-frequency influence of R_{esd}. Yet, they introduce an RHPZ, which can complicate phase margin requirements in fast-response designs. Despite these tradeoffs, both approaches can be tuned to achieve comparable gain and phase margin characteristics, as confirmed through SIMPLIS modeling and practical boost converter implementations.

Designers must weigh these attributes based on application-specific constraints such as startup behavior, transient response, and closed-loop bandwidth objectives. The derived expressions and validated models provide a solid foundation for informed selection and optimization of OTA-based compensation networks in next-generation power systems.

References

1. "A Type 3 OTA in the Compensation of a Voltage-Mode-Controlled Buck Converter" by Christophe Basso, Future Electronics, February 2023.
2. *Designing Control Loops for Linear and Switching Power Supplies* by Christophe Basso, Artech House, 2012, pp. 357-380.
3. "Enhanced OTA Models Improve Design Of Feedback Compensation Networks" by Alain Laprade, How2Power Today, July 2014.
4. NCP1034 onsemi datasheet.
5. NCV8871 onsemi datasheet.
6. NCV898031 onsemi datasheet.

About The Author

With more than 40 years of experience in power electronics, Alain Laprade has built a reputation for delivering practical, simulation-backed solutions across diverse power conversion platforms. His work spans automotive, industrial, and consumer applications, where he has specialized in analog control design, EMI mitigation, and component-level optimization for switched-mode power supplies.

In his last 15 years as an applications engineer at onsemi, Alain has supported design teams with clear, actionable guidance rooted in thorough analysis and real-world performance. His ability to synthesize complex feedback behaviors into usable design strategies continues to benefit engineers striving for efficiency and stability in high-performance systems.

Alain remains an active contributor to the engineering community through rigorous documentation review and technical mentoring. His experience in simulation environments and design validation offers a reliable compass for engineers navigating evolving semiconductor architectures and control methodologies. Whether reviewing technical literature or refining best practices, Alain is dedicated to promoting robust, resilient designs that meet the demands of modern power systems with clarity and precision.

For more on compensating power supplies, see How2Power's Design Guide, locate the "Design Area" category and select "Stability".